Structure of polystyrene glasses

G. R. Mitchell and A. H. Windle
Department of Metallurgy and Materials Science, University of Cambridge, Pembroke Street, Cambridge CB2 3QZ, UK
(Received 9 August 1983)

Wide-angle X-ray scattering from both unoriented and axially deformed glassy polystyrenes (atactic and quenched isotactic) is compared with that calculated for isolated molecules in different conformations. No satisfactory fit is obtained. It is apparent that the scattering beyond $s=1.0$ Å^{-1} is very similar to that from benzene and styrene, having a large contribution from contacts between phenyl groups attached to neighbouring molecules which are not represented in a single chain model. The only significant difference between the scattering of the polymer and the two low molecular weight liquids is that there is a small peak at $s=0.75$ Å^{-1} (0.62 Å^{-1} for the isotactic glass) which forms on polymerization and was first reported by Katz in 1927. For drawn samples the peak intensifies on the equator and apparently represents interchain correlations. However, in comparison with those of other non-crystalline polymers this interchain peak is weak, at a surprisingly low scattering angle in relation to the expected spacing of the chains and shows a very significant increase in intensity with increasing temperature. A model is proposed in which the phenyl groups segregate on a molecular scale to form stacks; there are fewer stacks than chain backbones and they have a low electron density core which expands considerably in relation to its small diameter as the sample temperature increases. The model accounts for the position and temperature sensitivity of the interchain 'polymerization' peak. It also shows some similarities to the organization of isotactic molecules in the crystalline state. The stacks of phenyl groups contribute to the X-ray pattern as if they were flexible superchains. The cylindrical distribution function derived from the scattering pattern of the oriented polymer indicates that the phenyl groups are in register in all directions over distances of the order of several chain diameters.

(Keywords: polystyrene glass; molecular conformation; X-ray scattering; molecular packing; phenyl groups)

INTRODUCTION

Polystyrene is unusual among non-crystalline polymers in that the wide-angle X-ray scattering (WAXS) shows a diffuse halo at $s=0.75$ Å^{-1}* which is completely absent from the scattering pattern of the monomer. In the early work of Katz[1,2] this halo was called the 'polymerization ring'. However, its presence in other polymers, although perhaps assumed, was only confirmed by Katz for polyindene and polycumarone. In fact, X-ray patterns of the majority of polymer glasses, rubbers and melts show no such ring. Plastic extension of polystyrene[1,3] leads to the intensification of the halo on the equator (i.e. normal to the extension axis), which indicates that it is associated with spatial correlations between chains.

It is arguable that over the years more X-ray studies have been made of polystyrene (PS) than any other non-crystalline polymer. However, determined attempts to measure its local conformation using WAXS analysis[4-6] have met with rather less success than in other polymers. It is noteworthy that it is in the nature of these analyses to place very little emphasis on information at low scattering angles. Thus, they take no significant account of the polymerization ring.

In some respects this paper follows the approach reported in previous studies. Reduced X-ray data are compared with scattering curves calculated for isolated molecules in a range of sterically possible conformations. Additionally, particular attention is given to the source of the polymerization ring and which is shown to be the key to understanding the organization of PS molecules in the glass.

* $s=4\pi \sin\theta/\lambda$

0032-3861/84/070906-15$03.00

EXPERIMENTAL

The atactic PS used in the study was BP grade KLP 35; the exact proportion of syndiotactic sequence is unknown, but n.m.r. measurements on similar materials suggests that the fraction of racemic dyads is 0.6[7]. The intensity data were recorded using counter diffractometers with (a) symmetrical reflection geometry and MoKα radiation to provide an s range of 0.2–13 Å^{-1} and (b) symmetrical transmission geometry, incident beam monochrometer, Eulerian cradle, temperature stage and CuKα radiation provided an s range of 0.2–6.2 Å^{-1}. The data were smoothed and corrected for polarization, multiple scattering and absorption, using the procedures detailed elsehwere[8,9]. For conformational studies it has proved useful to work with the reduced form, $i(s)$, of the fully corrected intensity curve $I_{corr}(s)$:

$$i(s)=kI_{corr}(s)-\sum_j f_j^2(s)-I_{comp}(s) \quad (1)$$

where $\sum_j f_j^2(s)$ is the independent scattering from one

chemical repeat unit, $I_{comp}(s)$ the Compton scattering and k the normalization factor. The s-weighted reduced intensity function $si(s)$ for atactic PS is shown in *Figure 1*. The most intense peak is at $s=1.4$ Å^{-1}, with other peaks at $s=0.75$, 3.1, 5.6, 9 and 10 Å^{-1}. The peak at $s=0.75$ Å^{-1}, which is Katz's polymerization ring, appears weak in this plot as a consequence of the data reduction and s weighting appropriate to an interference function.

As noted previously[4] the scattering from unoriented samples of a-PS and quenched i-PS is very similar. One difference, however, is that the interchain peak for the isotactic material is at a slightly lower angle, at $s=0.63$ Å^{-1} compared with 0.75 Å^{-1}.

The reduced s-weighted scattering for a-PS oriented at 85°C by extrusion in a channel die is shown in *Figure 2a*. The equatorial and meridional sections drawn in *Figure 2b* indicate the meridional nature of the most intense peak, and the equatorial intensification of the polymerization ring. The cylindrical distribution function (CDF), derived from the data of *Figure 2a*, using the method of Mitchell and Lovell[9], is shown in *Figure 3*. There is a strong meridional periodicity of 5 Å which is largely related to the most intense peak in the scattering function.

The procedures used in this work for analysing the scattering functions and the real space equivalents involve their comparison with similar functions calculated for sterically possible models. The method of calculating the scattering from a set of atom positions has been described previously[10,11].

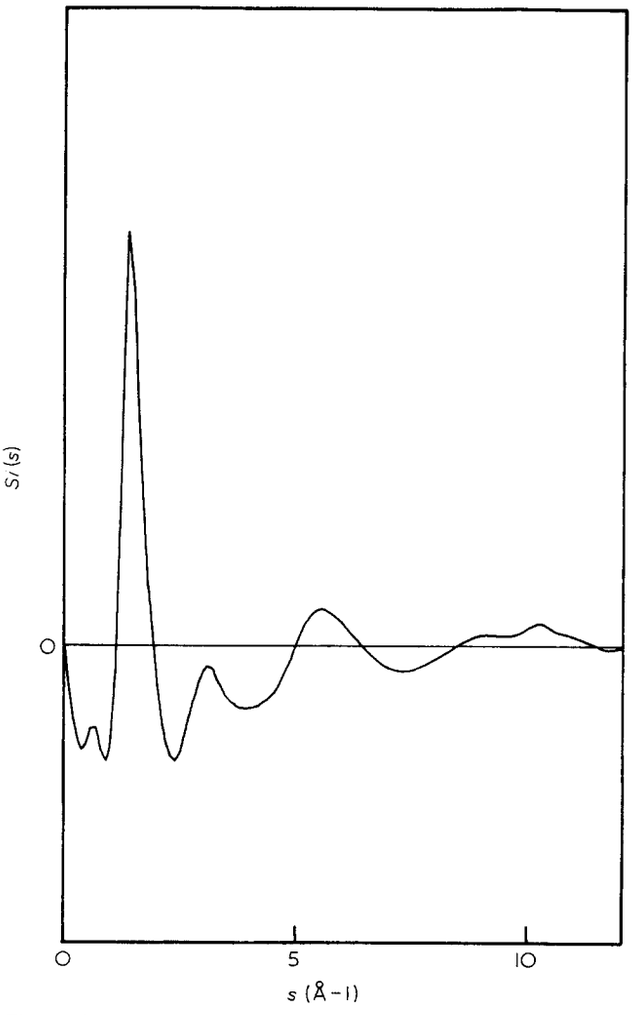

Figure 1 s-weighted reduction intensity function $si(s)$ of atactic polystyrene ($s=4\pi \sin\theta/\lambda$)

PREVIOUS WORK

Following the work of Katz, several authors have considered the WAXS of oriented a-PS, and the work of Milberg[12], Brady and Yeh[13], May[14,15], Colebrook and Windle[16] and Lovell and Windle[17], has all added to the evidence relating to the equatorial nature of the polymerization ring. Brady and Yeh additionally reported studies of the differing rates of orientational relaxation and retraction in cold drawn samples of a-PS annealed below T_g, and accounted for these ffects in terms of a bundle model. May's analysis[14,15] favours some sort of parallel chain assembly with disordered hexagonal packing, while Colebrooke and Windle[16] azimuthally-averaged the fibre patterns for a-PS and showed that the result was indistinguishable from the scattering of unoriented PS.

The variation of the WAXS pattern with temperature is a useful method for assessing the structural origin of features in the patterns. The most comprehensive of such studies was carried out by Kilian and Boueke[18] but similar results were also obtained by Krimm[19] and Lovell and Windle[17]. Kilian and Boueke observed that, whereas the intensity of the main halo at $s\sim1.5$ Å^{-1} was almost independent of temperature, the intensity of the first halo (the polymerization ring) increased markedly above T_g. Similar increases, though less marked, were observed for the angular position and breadth of the two peaks. Recently Schuback, Nagy and Heiss[20] have reported the effect of temperature on the radial distribution function (RDF) of PS. The only significant change recorded over a temperature range 20–180°C involved the peak at ≈10 Å, which shifted to slightly larger spacing. RDF's are reported in the literature derived from both electron diffraction data[21,22] and from X-ray scattering studies[4,23,24]. Wecker *et al.*[4], while noting the similarity in the scattering from i-PS and a-PS glasses, used a model RDF based on the crystal structures of i-PS to assign peaks in the RDF for $r>5$ Å as predominantly interchain, while they interpreted those peaks at $r\approx5$ Å in terms of phenyl–phenyl correlations of both inter and intrachain origin. A detailed conformational study of i-PS using WAXS was carried out by Adams *et al.*[5] and although their final model curve is in promising agreement with experimental observation, their conformational parameters are in direct conflict with those indicated by conformational energy calculations[25].

Small-angle neutron scattering (SANS) studies indicate that PS adopts random coil configurations in the glass[26,27], a result complemented by the depolarized light-scattering studies[28].

Semi-empirical conformational energy calculations provide a useful starting point for structural studies, and the results of several such calculations have been presented[25,29–34]. In some cases the rotation of the phenyl groups is considered[33,34], and it appears that unless sterically unfavourable backbone angles are adopted the rotation of these groups around the bonds connecting them to the backbone is restricted to a range $\pm20°$–$30°$ about the position where the plane of the group is normal to the chain direction. Panov *et al.*[30] stress the relevance

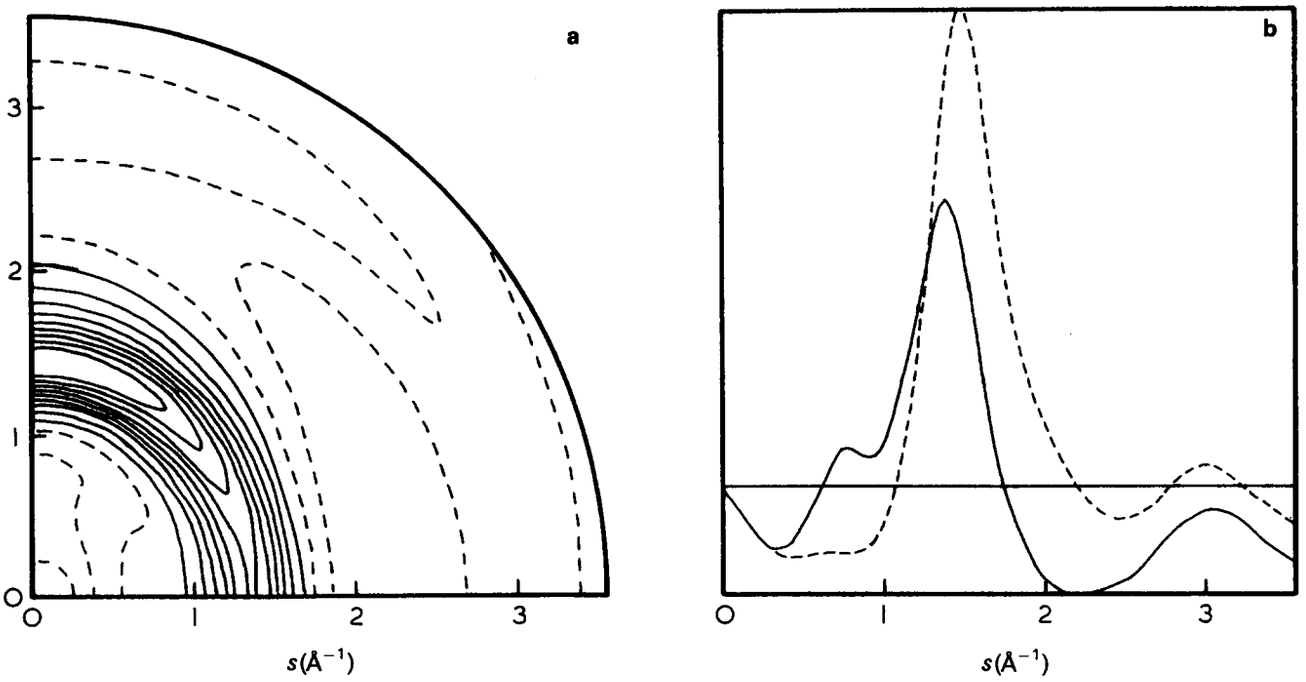

Figure 2 (a) s-weighted reduced intensity function $si(s, \alpha)$ for atactic polystyrene oriented at 358 K with an extension ratio 3. The extension axis is vertical and dashed contours represent negative values. (b) Plot of meridional (- - - -) and equatorial (——) sections of *Figure 2a*

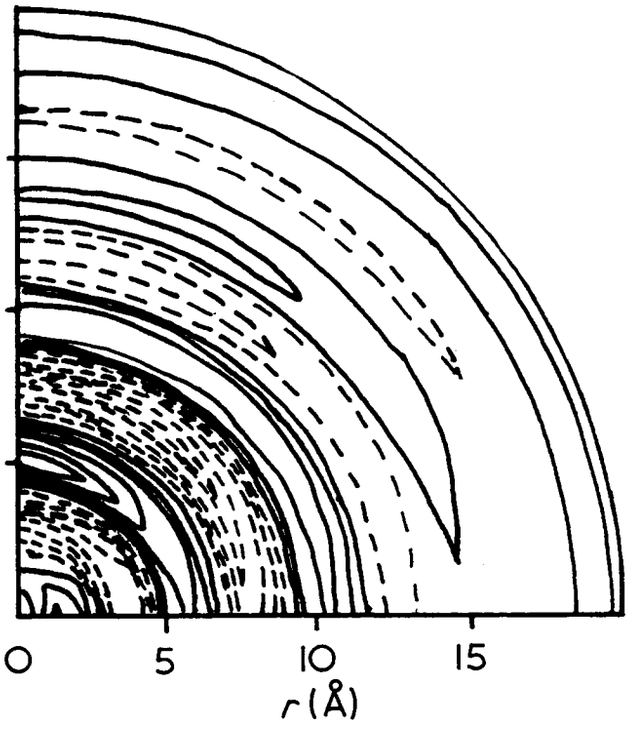

Figure 3 Cylindrical distribution function CDF derived from the intensity data shown in *Figure 2a*

of the intermolecular contribution to the stable conformation of the molecule while Yoon *et al.*[25] found it necessary to introduce a 'solvent' interaction parameter into their calculations. Overall these calculations show there to be low energy conformers involving sequences of *trans–trans*, *gauche–gauche*, and *trans–gauche* rotation states. It is noteworthy that the i-PS crystalline chain conformation, a 3/1 helix[33], corresponds to regular *trans–gauche* sequences. More recently, however, Atkins *et al.*[36] have reported a different crystal structure. It is produced by drawing gels based on non-aromatic solvents and features a near all-*trans* extended chain conformation.

CONFORMATION AND PACKING

In contrast to work on other non-crystalline polymers, conformational analysis of polystyrene using WAXS information has not been especially successful. It seems that the intrachain scattering calculated for model chains in any feasible conformation is always at variance with that observed experimentally[5,6]. It is possible that this lack of agreement stems from the assumption that the scattering observed at higher angles represents intrachain correlations alone. Whereas it appears that in the case of PS the imprint of the interchain correlations on the diffraction pattern cannot be so readily separated from the intrachain information.

On this basis alone polystyrene appears unusual. In the analysis which follows efforts are made to consider conformations which are as realistic as possible in their irregularity and also the effects of correlations between phenyl groups which are attached to different, but neighbouring, backbones.

Conformations of regular chains

For comparison, it is useful to look at examples of attempts to fit scattering calculated for particular regular conformational sequences to the data. *Figures 4a* and *4b* show intrachain reduced functions calculated for different run lengths of syndiotactic PS in $(tttt)_n$ and $(ttgg)_n$ conformations, respectively. In each case the calculated function is compared with that derived from experiment for a-PS (60% racemic dyads). These particular conformations were chosen as giving the closest fit with experiment; however, it is very clear that long persistent sequences (> 20 repeat units) are not present, and that the $(ttgg)_n$ sequence (5 repeat units) provides a better fit for

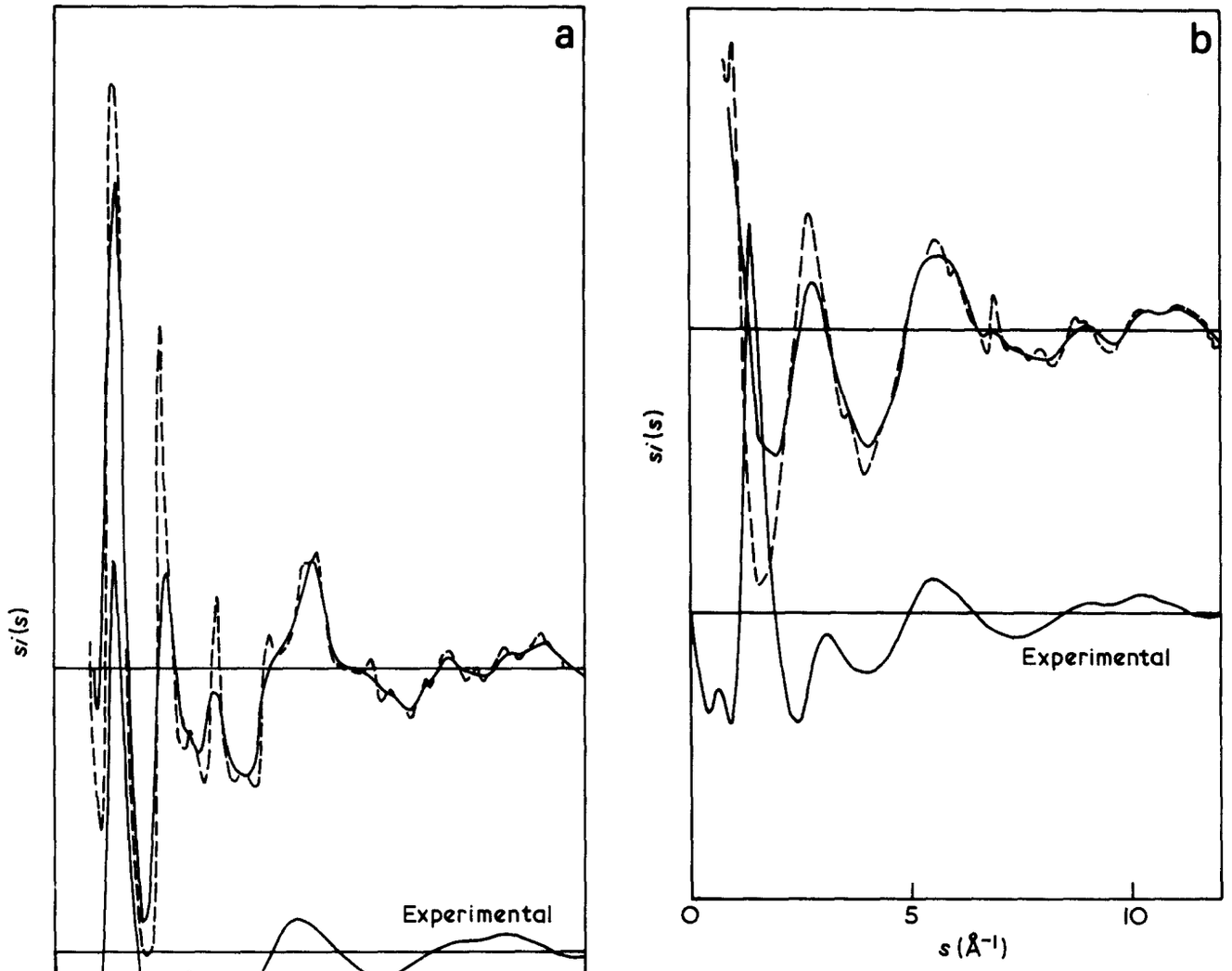

Figure 4 Calculated scattering function, $si(s)$, for syndiotactic PS chains comprising 10 backbone bands (——) and 40 backbone bands (- - - -). (a) An all-*trans* conformation $(tttt)_n$; (b) a $(ttgg)_n$ conformation. Each is compared with the experimental scattering curve of *Figure 1*

$s > 2.0$ Å^{-1}, although even this calculated curve contains a feature at $s = 7$ Å^{-1} not discernable in the experimental data.

It is apparent in the scattering patterns from oriented specimens (*Figure 2*) that the strongest halo, that at $s = 1.5$ Å^{-1}, has mixed meridional and equatorial character with the more intense scattering being on the meridian. Thus, the calculated curve for isolated chains would be expected to show also a definite peak at $s = 1.5$ Å^{-1}. Such a peak is apparent in the calculated scattering curve for $(tttt)_n$ (*Figure 4a*) but not in that for $(ttgg)_n$ (*Figure 4b*). Consequently, it is not possible to achieve any satisfactory fit, and the only rather vague suggestion possible at this stage is that the chain may contain a mixture of $(tttt)_n$ and $(ttgg)_n$ sequences, a proposal already recorded in the literature[17].

Figures 5a and *5b* show cylindrical distribution functions (CDF's) calculated for the same two regular sequences of s-PS. The method used was that of ref. 9 but with the average density calculated and removed by procedure outlined in ref. 8. The level of agreement of the (*tttt*) model with the experimental CDF (*Figure 3*) appears to reflect the dominant influence of the correlation between phenyl groups, as represented by the peak at $s = 1.5$ Å^{-1} in the scattering function, on the real space presentation of the data.

Conformations of irregular chains

To calculate the scattering from more realistic chains, sequences were built in the computer in which the probability of a racemic dyad was 0.6 and their distribution Bernoullian in accord with earlier observations[7]. The sequence of rotation states (*trans, gauche*) along the chain was random, but distributed in accord with the results of conformational energy calculations. The higher steric hindrance associated with backbone rotation angles in the negative *gauche* domain reduces the number of rotation states to 2 (*trans* 0° and *gauche* 110°). The

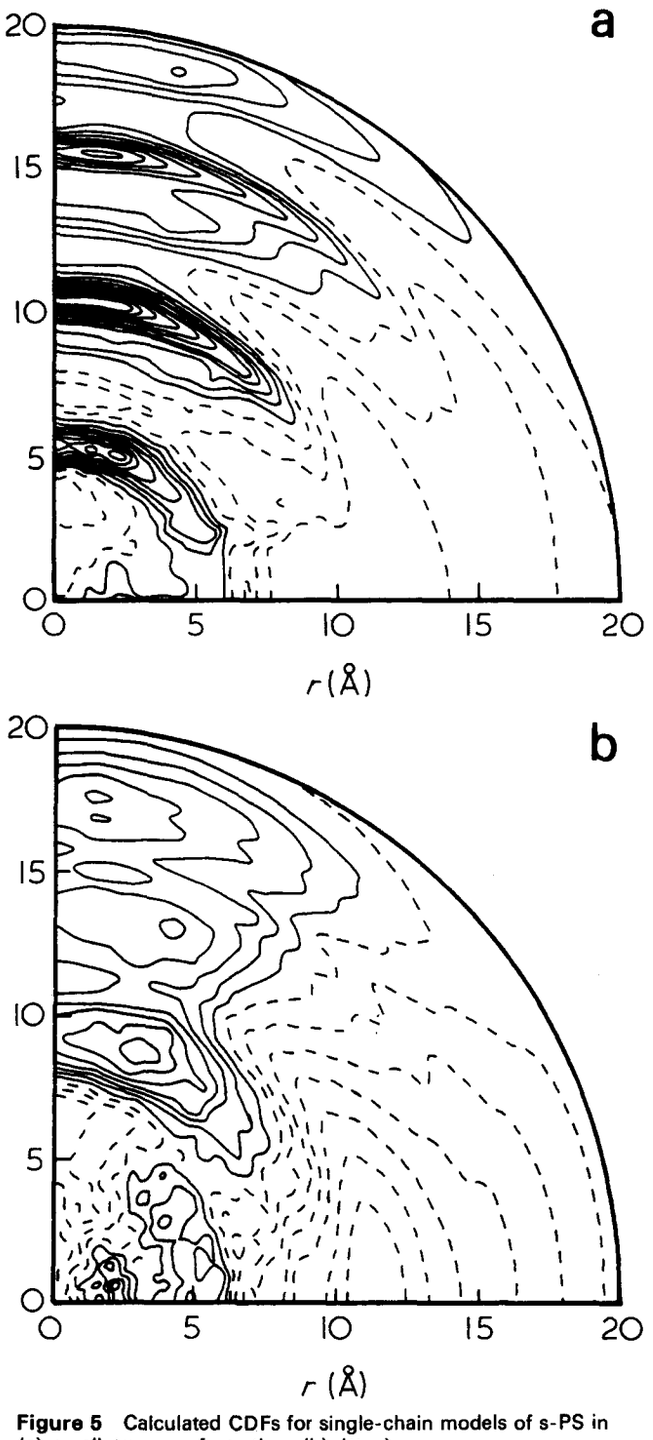

Figure 5 Calculated CDFs for single-chain models of s-PS in (a) an all-*trans* conformation; (b) $(ttgg)_n$

matrices defining the interdependence of rotation states are[25]:

$$U' = \begin{bmatrix} 1 & 1 \\ 1 & 0 \end{bmatrix} \tag{2}$$

which represents the statistical weights for the second-order interactions for the bonds flanking the substituted carbon atoms and indicates that the presence of phenyl groups, rules out *gg* but does not influence *tt* or *tg*. The U'' matrices express not only the first- and second-order interaction for the bonds within a dyad, but also the first-order interactions for bonds joining dyads. This slightly artificial partitioning arises purely from the mechanisms for deriving the statistical weights from energy maps:

$$U''_m = \begin{bmatrix} \omega'' & 1/\eta \\ 1/\eta & \omega/\eta^2 \end{bmatrix} \tag{3a}$$

$$U''_r = \begin{bmatrix} 1 & \omega'/\eta \\ \omega'/\eta & 1/\eta^2 \end{bmatrix} \tag{3b}$$

The statistical weight η is related to an energy E_η by:

$$\eta = \eta_0 \exp(-E_\eta/RT) \tag{4}$$

The values of η_0 and E_η and the equivalent factors for the other weights may be obtained from conformational energy calculations through a series of simultaneous equations[25]. The calculations of Yoon and Flory[25] showed that ω and ω' which represent the second-order interactions between CH_2–CH_2 and CH_2–C_6H_5, respectively, may be considered to be the same and equal to $1.3\exp(-1000/T)$, i.e. at 398 K, $\omega = 0.105$. The values ascribed to η, the first-order parameter expressing the statistical weight of *trans* relative to *gauche* and to ω'' the second-order interaction by neighbouring phenyls, are markedly dependent upon the assumed model for the intermolecular interactions. Here, chains built using a range of values for $E_{\omega''}$ and E_η are considered which span those chosen by Yoon and Flory[38] ($E_{\omega''} = 2.2$ kcal; $E_\eta = 0.8$ kcal), as providing the best fit to chain trajectories measured in solution and confirmed by neutron scattering.

To assign a sequence of rotation states randomly but in accord with this scheme requires conditional probabilities rather than statistical weights. The probabilities may be determined using procedures described by Flory[37], and the scattering calculated for chains with random distributions of rotation states derived using such techniques are shown in *Figures 6a* and *6b*. The agreement between calculated and experimental $si(s)$ curves is slightly better than that seen for regular chains. However, it still is not completely satisfactory. It may be possible to obtain smoother calculated curves by allowing some variation in the backbone rotation angle assigned to each rotation state, but the significant aspect is that substantial changes to the energy weightings and thus backbone conformation, have comparatively little effect on the curve beyond $s = 2$ Å^{-1}, where fixed bond distances within the phenyl groups will largely determine the general form. The greatest sensitivity to conformation is found in the interphenyl peak at 1.5 Å^{-1}, although quantitative comparison with the corresponding experimental peak is not possible, presumably because of substantial contributions to this peak from correlations between phenyl belonging to adjacent chains.

The fact that PS does not readily yield to the established type of X-ray conformational analysis is interesting in itself. It also suggests the need for a different approach.

Assemblies of phenyl groups

As the phenyl groups tend to dominate the calculated scattering curves for isolated chains of PS, it is perhaps more useful to consider the bulk polymer as an assembly of phenyl groups linked together by the relatively insignificant (as far as X-ray scattering is concerned) carbon backbones.

An indication of the relevance of such an approach is

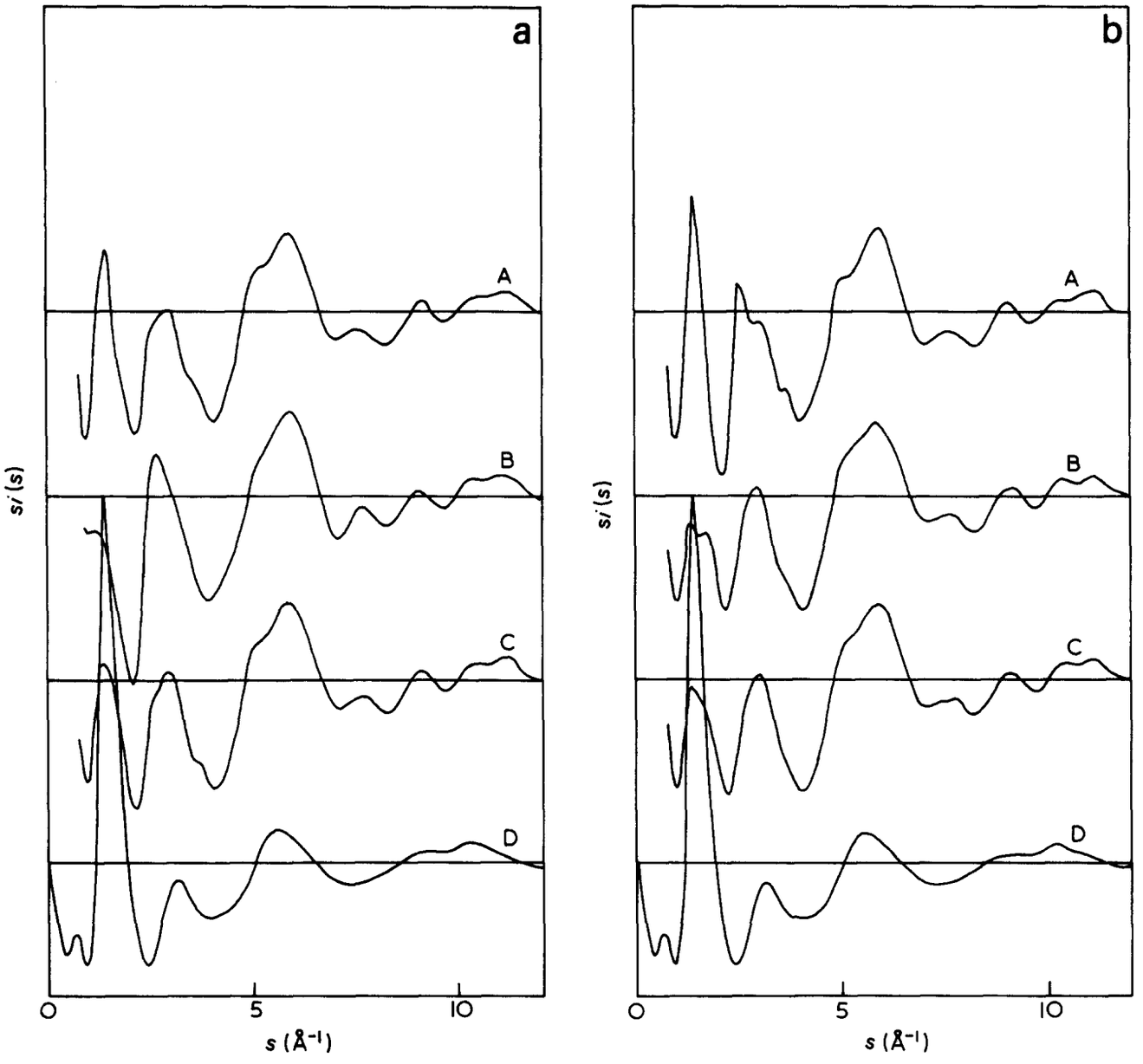

Figure 6 Intensity functions $si(s)$ calculated for random atactic polystyrene chains with a racemic dyad probability of 0.6. The assignment of rotation states was determined on the basis of statistical weight matrices describes in the text for a range of values of E_η and $E_{\omega''}$. (a) With E_η constant at 0.4 kcal and varying $E_{\omega''}$. $E_{\omega''}$; A, 3.0; B, 0.0; C, 2.2 kcal; D, experimental. (b) With $E_{\omega''}$ constant at 2.2 kcal and varying E_η. E_η: A, 1.0; B, 0.0; C, 0.4 kcal; D, experimental

provided by the comparison of the scattering curve of liquid styrene with that of a-PS made in *Figure 7*. At >1 Å^{-1} the curves are very similar, although the differences which are apparent are themselves significant. The most intense peak at $s=1.5$ Å^{-1} is sharper for a-PS than for styrene possibly indicating a slightly greater packing order in the polymer[39]. At <1 Å^{-1} the notable difference is, of course, of the peak at $s=0.75$ Å^{-1} in the scattering from polystyrene which is not present in the monomer curve. In *Figure 8* the $si(s)$ curve for a-PS is compared with that of benzene, the latter derived from the work of Narten[40]. The main peak at 1.5 Å^{-1} for benzene is slightly sharper than for a-PS, and also shows a shoulder at 1.9 Å^{-1} related to short-range face-to-face correlations of the aromatic rings. The absence of this shoulder from the PS curve may indicate that attachment of the phenyl groups to the backbone prevents such close contacts, although it should be noted that in PS oriented by drawing, the planes of the phenyls tend to lie normal to the extension direction[16]. Overall, the similarity of the scattering curves at $s>1$ Å^{-1} indicates that the phenyl–phenyl contacts are as dominant in the polymer as they are in the monomer and in benzene. The implications of the comparison between the scattering of styrene, benzene and a-PS are underlined by an examination of the calculated scattering from an assemblage of randomly-packed phenyl groups. Specific orientation correlations are not included in the model, and the interphenyl positional correlations are represented by the isotropic interactions between randomly but close-packed spheres. The scattering calculation procedure is that developed to model the packing of polyethylene segments and is discussed in detail elsewhere[11]. Account is taken of the 'softness' and shape anisotropies of the units by utilizing a

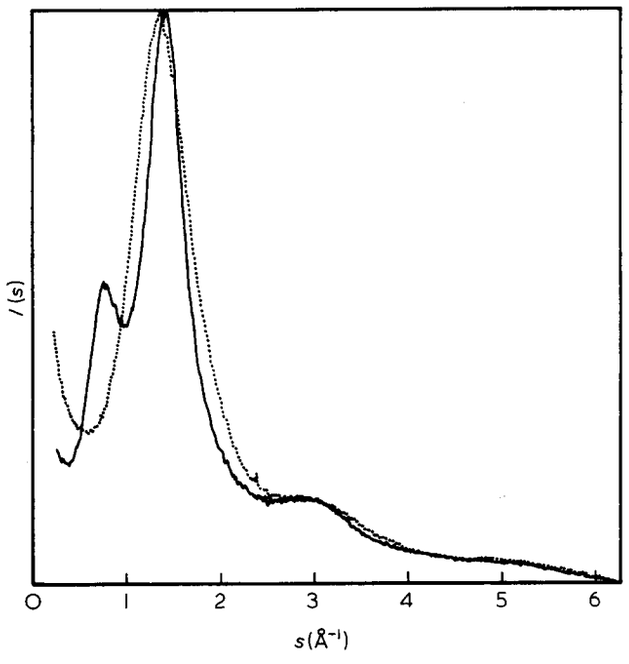

Figure 7 The intensity function $I(s)$ for a-PS (—) compared with that of liquid styrene (·····) at room temperature

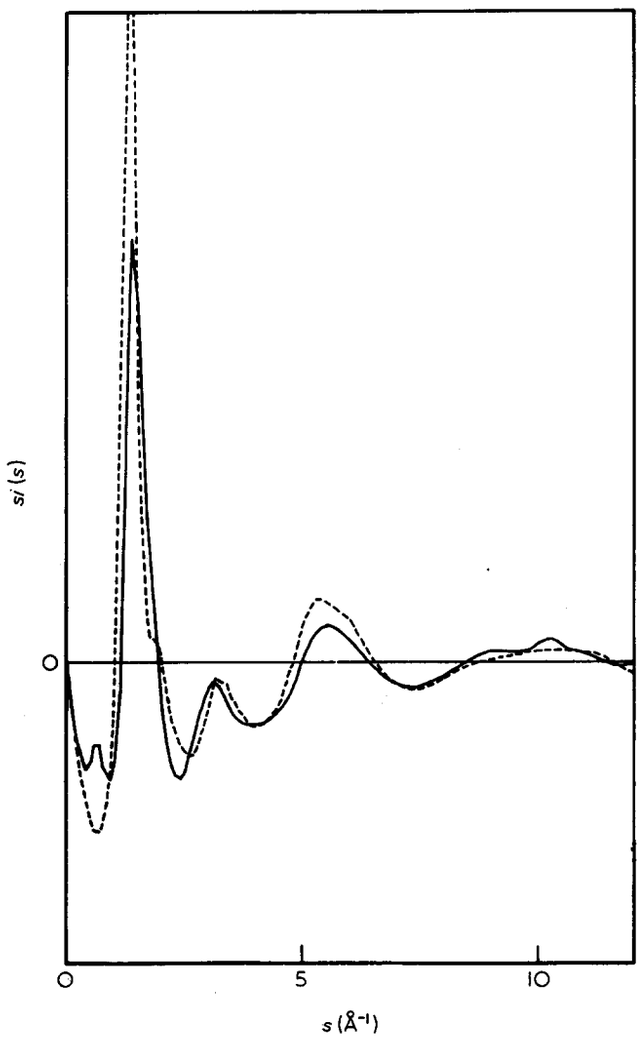

Figure 8 The reduced intensity function $si(s)$ for a-PS (——) compared with that of liquid benzene (- - - -) (derived from the work of Narten[40])

distribution of sphere sizes as shown in the insert to *Figure 9*. The main curve of the figure is the scattering, as an $si(s)$ function, calculated for the model of randomly-packed phenyl groups. The shoulder which is present in the main peak of benzene at $s=1.9$ Å^{-1} is absent as a consequence of the omission of local orientational correlation from the model. However, the agreement with the experimental scattering from a-PS, in all respects except that of the polymerization peak at $s=0.75$ Å^{-1}, is notable.

The structural implications of the scattering for $s > 1.0$ Å^{-1}

The linking of the phenyl groups by the backbone carbon atoms to form a chain assembly introduces an additional level of spatial correlation, albeit in only one direction. The effects of this correlation upon the structure and the consequent scattering patterns depends on whether the relative position of the side groups is controlled by a tendency to maximize intrachain order or whether it is determined more by the necessity of achieving good packing with other such groups on neighbouring as well as the same chain. For a polymer such as PS with substantial side groups (the side groups account for 75% of the material), it is perhaps not surprising that polymerization has little effect upon the scattering curve at ≈ 1 Å^{-1}. This observation, however, implies that the PS backbone does not hold any persistent conformation for more than a few bonds, and also that the side groups along any one chain are not specially associated, but have every opportunity to form contacts with groups belonging to adjacent molecules. Such a model is supported by the semi-empirical conformational energy calculations for PS[25] which require a 'solvent

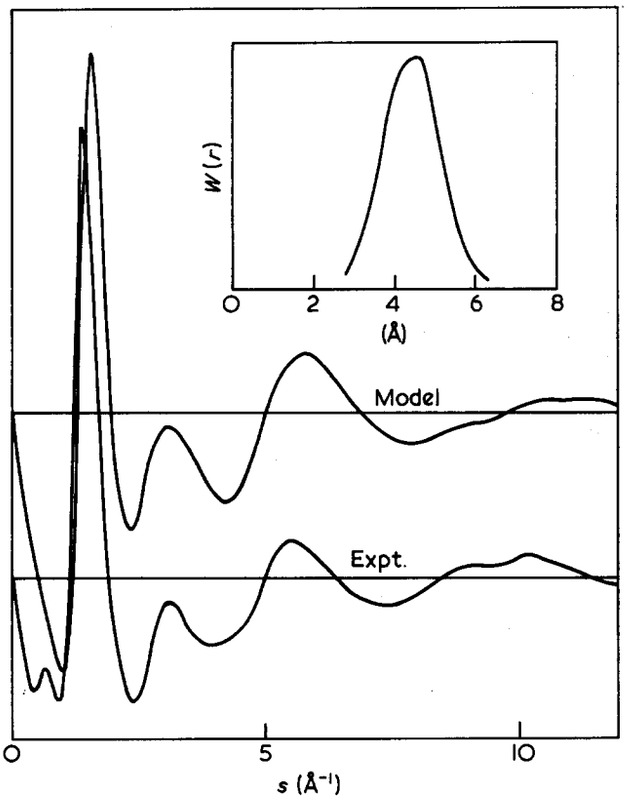

Figure 9 The calculated reduced intensity function $si(s)$ for a model of randomly-packed phenyl groups with *no* orientation correlations compared with the experimental function for a-PS. The insert shows the distribution of sphere sizes used in the calculations

parameter' to take account of the open nature of the PS chain and the conformationally sensitive interactions with its environment.

It is noteworthy that this model contrasts markedly with that of polymethylmethacrylate (PMMA), in which the neighbouring side groups of any one chain are associated closely with each other and lock the backbone into significant sequences of one underlying conformation[10]. Correspondingly, there are intramolecular peaks in the scattering patterns of PMMA at $s = 1.5$ Å^{-1} and 2.1 Å^{-1} which are not present in the scattering pattern of the monomer[41] and represent correlations in side group positions determined by their attachment to the backbone.

The 'interchain' peak

For many non-crystalline polymers the lowest angle peak in the scattering curve is the most intense. It represents spatial correlations between segments of neighbouring chains and consequently concentrates on the equator in the scattering patterns of drawn samples. It is also, usually, at much the same position as the peak observed in scattering from the corresponding monomer which represents primary intermolecular correlations. Polystyrene is different. The lowest angle peak indeed intensifies on the equator for drawn samples, but it is comparatively weak and appears at a much lower angle than that of the intermolecular peak for the monomer. In fact it appears on polymerization at an angle at which there is minimal scattering for the monomer. It is also unusual in that it increases significantly in intensity with increasing temperature, markedly so above the glass transition temperature[18,42]. This behaviour is shown in *Figure 10*, in which curves for 20 and 250°C are compared. Apart from the large change in the first peak, the scattering is otherwise little affected by temperature. By way of contrast the substantial interchain peaks of PMMA or polycarbonate (for example) show only a marginal increase in intensity with increasing temperature.

Packing of overlapping chains. The weakness of the low-angle peak which appears on polymerization implies a lack of electron density contrast between the units responsible for it and, in structural terms, an interpenetration of the individual molecular envelopes. The lack of any support from the conformational studies presented previously for regular sequences of backbone rotation angles, leads to the general view of a random chain in which the side groups protrude in various directions from the chain backbone. In cross-section the chain can be considered to have a penetrable envelope of radius R surrounding an impenetrable core of radius R'. The chains are thus able to approach to give an inter-backbone distance of $2r^*$ where $r^* = (R + R')/2$.

On the assumption that a model of overlapping chains is the most appropriate for PS in a random conformation, it is important to explore the implications of molecular interpenetration for local packing geometry. As a first step a parallel model is considered. In no way does this imply that there is thought to be any significant parallelism in the unoriented PS glasses, but it does provide a starting point to consider possible packing densities which are not likely to be greatly different between parallel and random packing of flexible molecules. (Crystalline densities are usually only 5–15% greater than those of the corresponding glasses).

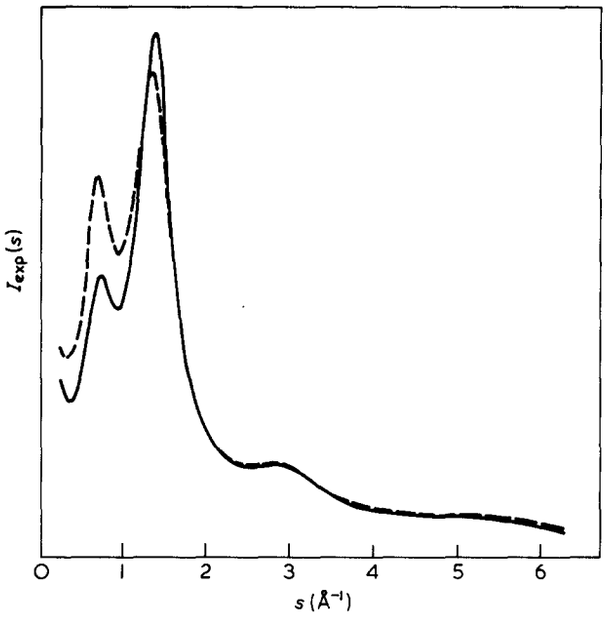

Figure 10 The measured intensity function $I(s)$ of atactic PS at 20°C (—) and 250°C (- - - -)

For parallel packing, it is possible to relate the minimum radius of a chain r^* to the packing density, ρ^*, of discs of radius r^* in the plane normal to the chain axes, and the observed macroscopic density ρ by:

$$\rho^* = r^{*2} L_m \rho N_A / M_m \quad (5)$$

where L_m is the distance along the chain backbone corresponding to each repeat chemical unit, N_A is the Avogadro number and M_m the molecular weight of each chemical repeat unit. Estimates of values for the parameters of the right-hand side of equation (5) are given in *Table 1*. The value for r^* is the best estimate based on known molecular and atomic dimensions, also it is difficult to assign a precise value to L_m, for a random PS chain, but realistic limits would place 2.1 Å $< L_m <$ 2.5 Å.

The substitution of the values from *Table 1* into equation (5), gives a two-dimensional packing fraction for overlapping PS chains of 0.54 (−0.12, +0.13). Even considering the generous limits, this packing density is, for chains, very low. It is instructive to compare it with values listed in *Table 2* obtained for possible models of packing based on the regular two-dimensional lattices shown in *Figure 11*. The agreement appears best with the model in which the co-ordination for overlapping PS chains is three fold. The implication of three-fold co-ordination is that although the spacing of the individual neighbouring chains is not necessarily greater than that assumed by the other packing modes, the two-dimensional lattice is

Table 1 Parameters assigned for polystyrene for use with equation (5). Definitions in text.

	Values assigned for PS
r^*	3.5 Å ± 0.25 Å
ρ	1.05 g cm^{-3}
L_m	2.3 Å ± 0.2 Å
M_m	104

Table 2 Packing density, ρ^*, and position of first-order diffraction peaks, s_p, for the models shown in *Figure 11*

Model	Co-ordination	ρ^*	Position of first order diffraction peak, s_p, as a function of r^*
a	6	0.91	$2\pi/r^*\sqrt{3}$
b	4	0.78	π/r^*
c	3	0.61	$2\pi/3^*r$

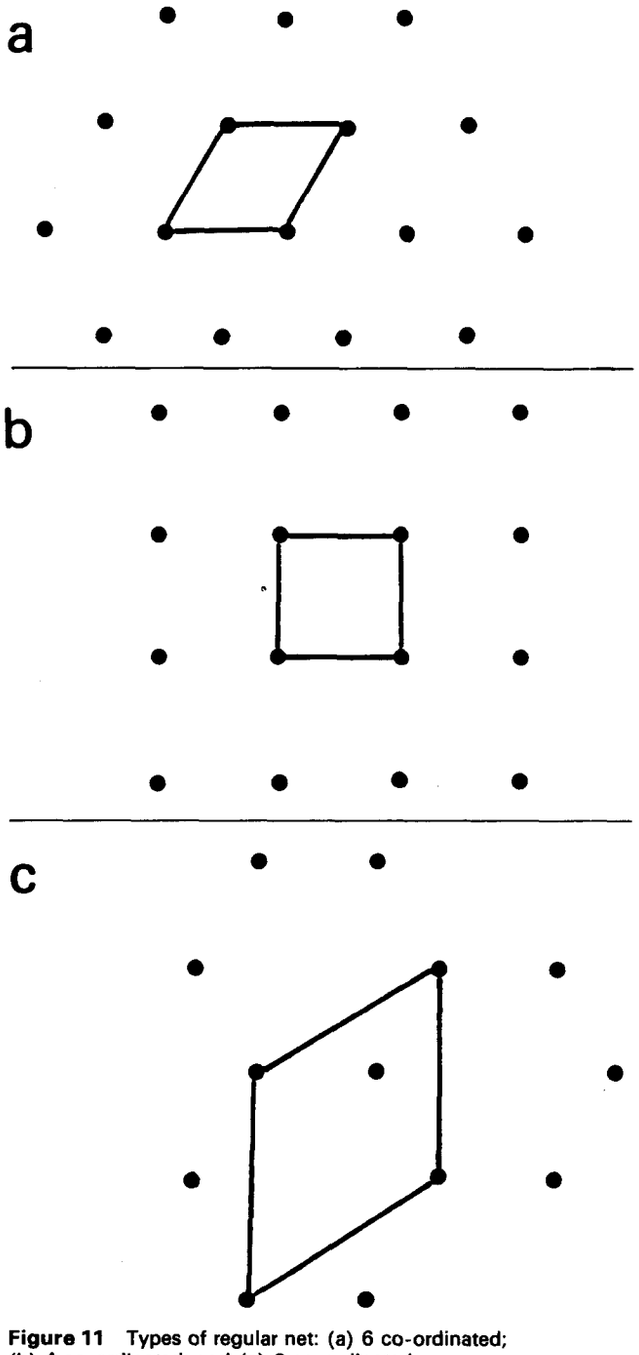

Figure 11 Types of regular net: (a) 6 co-ordinated; (b) 4 co-ordinated; and (c) 3 co-ordinated

larger, there being two chains per lattice point. In qualitative terms then, the idea of overlapping chains not only accounts for the weakness of the equatorial polymerization peak in PS, but also by virtue of the implication of three-fold coordination and the presence of two chains per lattice point, explains why the peak is at an unusually low angle and appears where no peak appears in the scattering from the monomer.

Figure 12 provides a cross comparison between the three ordered models for parallel packing, and measurements of the position of the polymerization ring and estimates of the closeness of approach of interlocking polystyrene molecules. The three sloping portions of curves cover values of r^* calculated, using equation (5), from the packing densities appropriate to each of the packing models a, b and c (see *Table 2*), the reported macroscopic density and an estimate of the axial length of each chemical repeat. The uncertainty in this last parameter leads (via equation (5)) to the range of r^* depicted for each model. The corresponding values of estimated peak position, s_p, are determined from r^* using the relations listed in *Table 2*. The horizontal bars represent the measured peak positions for i-PS and a-PS, and the range of r^* which appears commensurate with known molecular dimensions. Despite the uncertainty stemming from model calculations which are for regular packing on a two-dimensional net, it is possible to come on two complementary conclusions.

Firstly, if the chains overlap as would be expected on the basis of the estimated radii of the backbone and the backbone plus side group, then the nearest neighbour coordination number will be in the region of three. Secondly, a nearest neighbour coordination of three, which corresponds to a hexagonal net with one lattice point in three removed, and the unit spacing thus increased, seems to be the only packing able to account for the angle at which the PS interunit peak is observed for the quenched isotactic material. For the atactic polymer, although consideration of molecular dimension would

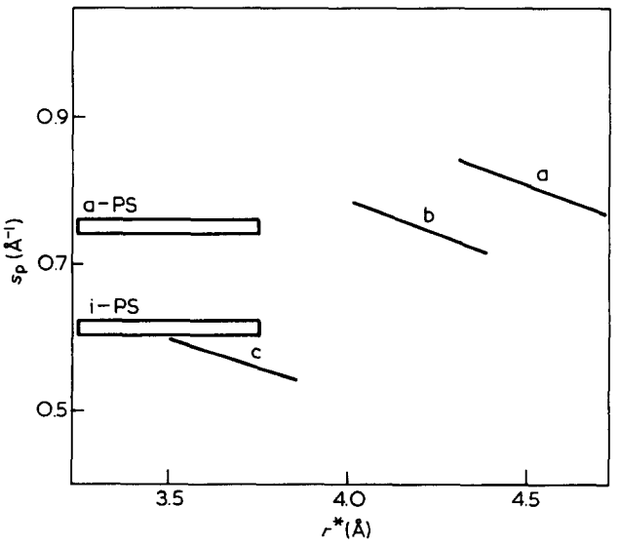

Figure 12 The relation between effective chain diameter and position of diffraction peak determined for the models of *Figure 11* compared with experimental estimates. The sloping lines on this diagram represent the values of the packing radius r^* and the corresponding position of the first-order diffracting maxima s_p calculated from equation (5) for each of the three packing modes of *Figure 11*. The horizontal range of the lines is related to the uncertainty in estimating the length of the chemical repeat unit projected onto the axis. The horizontal bars depict information available, independent of the models: the estimate of r^* based on consideration of known molecular dimensions, and the measured position of the interchain peak in the X-ray scattering

also suggest three-fold coordination, the higher angle at which the interchain peak is observed indicates that there is also a component of 4-fold type packing.

Relation to the scattering from the crystalline phase of i-PS. The crystal structure for i-PS was derived by Natta *et al.*[35] from X-ray diffraction of fibres. The chain conformation is a 3/1 helix and the chains are arranged in a rhombohedral cell (on hexagonal axes $a=21.9$ Å, $c=6.65$ Å) with either an R3C or an R$\bar{3}$C space group. A projection of the carbon atom positions and electron density contours onto the base plane is shown in *Figure 13*. The contours shown are calculated by ascribing to each atom a Gaussian electron density distribution.

The WAXS curve for a partially crystalline i-PS sample is shown in *Figure 14* where it is compared with that from the original quenched glassy material. The crystalline peak, indexed (110), is the primary, that is lowest angle, reflection from the hexagonal lattice which contains two chains per lattice point. Each lattice point is associated with a stack of phenyl groups contributed from six surrounding chains. The centres of the stacks are apparently regions of comparatively low electron density.

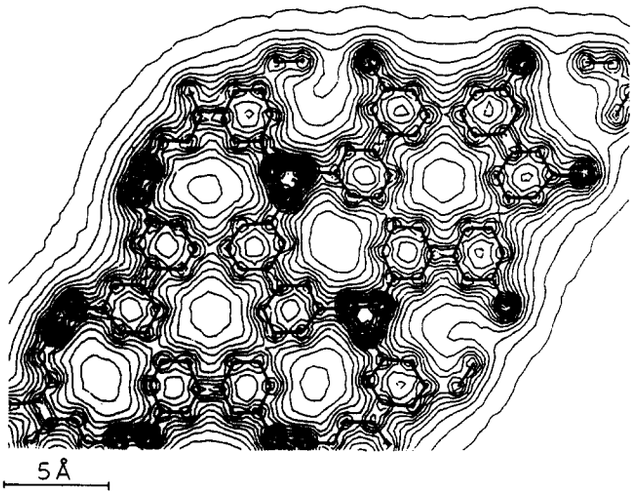

Figure 13 A projection of the crystal structure of i-PS onto the basal plane[35]. The contours show the relative levels of electron density in the projection

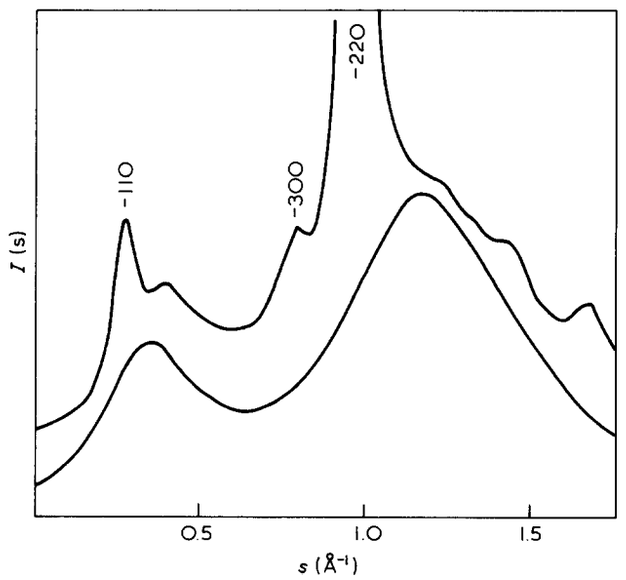

Figure 14 The intensity curves for a partially crystalline sample of i-PS compared with that for a quenched i-PS sample[42]

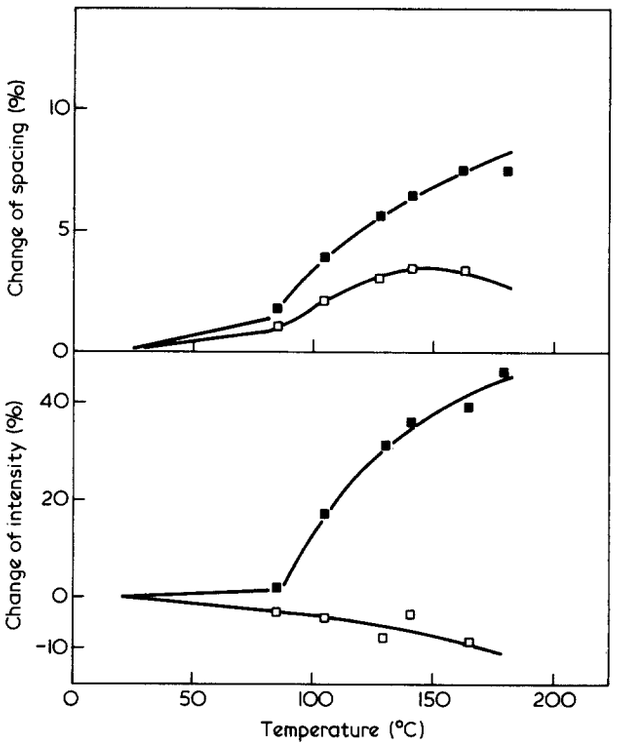

Figure 15 The effect of temperature on the scattering from a-PS in terms of peak shifts and intensity changes[17,42]. The first halo (■) is the polymerization peak at $s=0.75$ Å^{-1} and the second (□) is that at $s=1.5$ Å^{-1}

It is significant that the (110) reflection is at much the same angle as the first interchain peak in the scattering from quenched isotactic or atactic material. One straightforward interpretation of this observation would be that the phenyl grouping into stacks characteristic of the i-PS crystal is also a feature of the polymer structure in the melt or glass.

The effect of temperature on the interchain peak. The unusual effect of temperature on the interchain 'polymerization' peak has already been noted (*Figure 10*). It is now considered in detail. The principal consequence of increasing temperature on the scattering pattern of PS is a marked increase in intensity of the interchain peak at $s=0.75$ Å^{-1} (a-PS). This change in intensity is plotted against temperature in *Figure 15*, as is the change in the molecular spacing as measured from peak position. The fact that there is no significant effect of temperature on the remainder of the scattering and in particular on peaks shapes or widths (see *Figure 10*), indicates that the polymer expands without any general structural reorganization. To understand the particular temperature sensitivity of the interchain peak, it is useful to consider the general factors which relate peak intensity to temperature. In all materials, crystalline and non-crystalline, a decrease in peak intensity with increasing temperature will result from both an increase in thermal disorder and a reduction in electron density due to thermal expansion. There is no reason to assume that polystyrene structures should be immune from these effects, and so the changes which are responsible for an increase in peak intensity with temperature must presumably compensate and override them. For a system of units with no orientational

correlations, the intensity observed at a particular scattering vector may be considered as the product of the transform of the unit $F^2(s)$ and a 'sampling' structure factor $G(s)$ related to the spatial disposition of the units:

$$I(s) = F^2(s) . G(s) \quad (6)$$

If it assumed that the structure of each unit and, hence, its transform remains substantially unaffected by temperature variations, then the result of substantially unaffected by temperature variations, then the result of increasing temperature is to simply move the peak in the sampling function to lower scattering vectors as the distance bewteen the units increases. This effect, by itself, can account for an increase in peak intensity with temperature, although the magnitude of the observed effect implies that the structural units which give rise to the 'polymerization' peak, have a transform which has a relatively rapid change in intensity in the region where it is sampled.

To investigate the nature of a structure compatible with the large observed increases, it is necessary to consider the vehaviour of simple model systems. In a one-dimensional model, the variation in electron density can be represented by a 'top-hat' function of width $2a$, and thus the intrachain scattering function for a unit containing a fixed number of electrons is given by:

$$F^2(s) \propto [\sin sa/sa]^2 \quad (7)$$

Making the assumption that, for the small peak position movement involved, the sampling structure factor remains constant, the measured intensity will be:

$$I(s) \propto F^2(s) \quad (8)$$

The minimum spacing between the top hats is $2a$ and corresponds to a maximum scattering vector s_{max}, of $2\pi/2a$. It is convenient to consider the sampling postion for a top hat spacing of d as a fraction (q) of this maximum scattering vector, hence:

$$q = s/s_{max} = (2\pi/d).(2a/2\pi) = 2a/d \quad (9)$$

The relation given in equation (8) does not take account of the effect of increasing spacing upon the overall electron density. As the number of electrons associated with each unit is constant, the electron density is proportional to the reciprocal of the spacing of the units, and to q (as $q = 2a/d$ and a is fixed). A plot of $qI(q)$ for a system of top hats of fixed width $2a$ is shown in *Figure 16*. The intensity is zero when the units touch at $q = 1$ ($d = 2a$) or when spaced at infinity, $q = 0$. To relate the variation of intensity with sampling position to those variations ovserved experimentally, the first derivative of the function $qI(q)$ is considered with respect to q, normalized to $I(q)$, which describes the relative peak intensity as a function of q. A plot of the function $(d[qI(q)]/dq).(1/I(q))$ is shown in *Figure 17*. The curve may be divided into three regions as indicated on the Figure. The large central region (II) provides relatively small intensity changes for large movements in the peak position as the unit spacing is changed. In contrast, the regions corresponding to closely-packed structures (III) or very open structures (I), indicate that a large relative intensity change would be expected for small changes in peak position. For an intensity increase this model requires an *expansion* of the spacing between units (i.e. a reduction in q) in region III and a reduction in the spacing in region I. It is apparent from this one-dimensional model that a substantial increase in peak intensity with temperature can only be a property of very 'close packed' functions where d is only slightly greater than $2a$, especially considering the necessity to compensate for thermal disorder.

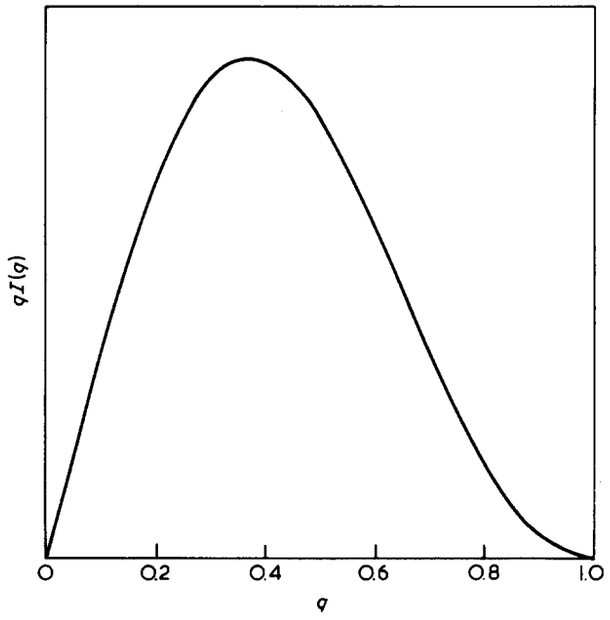

Figure 16 Plot of $qI(q)$ for a one-dimensional top-hat model, q is proportional to the reciprocal of the spacing of the units

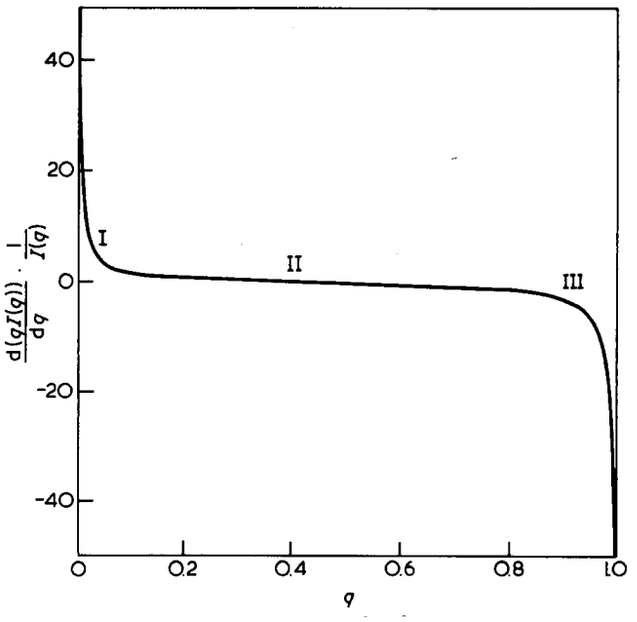

Figure 17 Plot of first derivative of the curve shown in *Figure 16* normalized to $I(q)$. The curve represents the relative intensity changes for an expansion of fixed size units

It is now necessary to consider assemblages of cylinders and spheres as models more relevant to the non-crystalline state. The structure factor for spheres and infinitely long cylinders have been given by Guinier and Fournet[43]. For spheres and cylinders the closest distance of approach is dependent upon both the size of the units and their spatial distribution. For cylinders (radius r) maximum density is achieved with a hexagonal packing

arrangement and, hence, the maximum sampling position will correspond to the Bragg reflections from the $\{1\bar{1}00\}$ form and $s_{max}=2\pi/\sqrt{3}r$. For spheres (radius r), the face-centred cubic and ideal hexagonal close-packed structures provide the closest packing and thus the maximum sampling position corresponds to the Bragg reflection from $\{111\}$ cubic and $\{0001\}$ hexagonal: i.e. $s_{max}=(2\pi\sqrt{3})/(2\sqrt{2}r)$.

The factor q is thus determined for two or three dimensions using the appropriate value for s_{max}. Assuming that diffraction occurs from a constant volume of the sample, the overall reduction in electron density on thermal expansion may be accounted for by weighting $I(s)$ with a factor of $1/(2r)^2$, or q^2, for cylinders and $1/(2r)^3$, or q^3, for spheres. Plots of the function $q^2I(q)$ for cylinders and $q^3I(q)$ for spheres are shown in *Figure 18*. The basic shape of the curves is similar to that for the top-hat function. For these two systems close packing does not provide a packing density of unity and hence there is a finite intensity for each close-packed structure. The sphere assemblange having a lower packing density ($\rho=0.74$) than cylinders ($\rho=0.91$), exhibits a greater intensity for $q=1$. *Figure 19* shows the derivatives of the curves in *Figure 19* normalized with $1/I(q)$. This Figure, as with *Figure 17*, indicates the relative intensity change that would be expected if the component units (cylinders or spheres) were moved apart without changing the size of the units.

In comparison with the equivalent curve for the top-hat functions, the regions I and II are very similar for both spheres and cylinders. However, the intensity changes predicted for structures in region III are less than those for the one-dimensional structures particularly so for the assemblages of spheres. The value of the normalized derivative function for $q=1$ is ≈ 5 (cylinders) and ≈ 1.5 (spheres). These values are the maximum possible, a real structure would also contain thermal disorder and smearing of the electron density, which would counteract the intensity increases. In addition the absence of second- and higher-order diffraction peaks for the polymerization

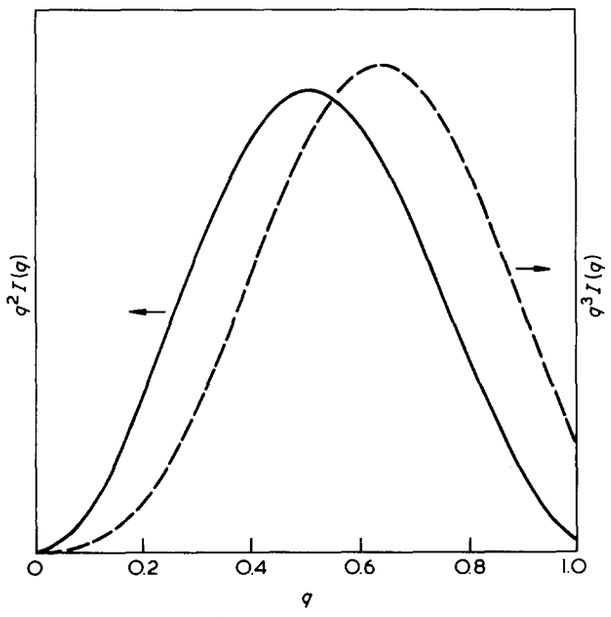

Figure 18 Plots of $q^2I(q)$ for the cylinder model (———), and $q^3I(q)$ for the sphere model (– – –)

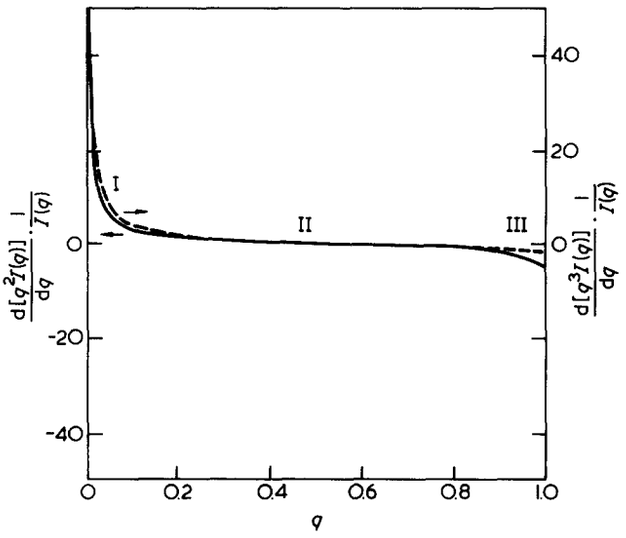

Figure 19 The normalized derivatives of the curves in *Figure 18*

peak indicates a random, disordered mode of packing, resulting in a lower maximum q value of the order of 0.95 for cylinders and 0.92 for spheres. The corresponding values of the normalized derivatives are thus ≈ 2 for cylinders for cylinders and ≈ 1 for spheres. The experimental value of the normalized derivative function for a-PS is 6 ± 1. Such a value is not possible for the expansion of a closely-packed system of either cylinders or spheres in region III.

However, region I (*cf. Figure 19*) which corresponds to dilute systems, does have the potential of describing the observed rapid change in peak intensity, albeit in the wrong sense. For the cylinder model a ratio of the spacing to diameter of the units of 20 would suffice, and for the sphere model 14. At first sight such a prediction, depending on an increase in q, would seen to require a contraction of the unit spacing with increasing temperature, which of course does not occur. But that is because the size of the units has been considered to be fixed, the effect of temperature being limited to an increase in the separation of the units. However, an increase in the ratio q $(=2r/d)$ can also be attained if the factor $2r$ is allowed to increase more rapidly than d, for example, a simple affine expansion gives $q=(2r+\delta)/(d+\delta)$ a ratio greater than $2r/d$ for positive δ. Before evaluating more precisely the intensity increase expected for such a model, it is appropriate to consider what structural features might correspond to such widely-spaced units.

The units required are small in comparison with their spacing. If the spacing is 10 Å then the diameter of the units will be of the order of 0.5–1.0 Å. It is instinctive to associate such a feature with the chain backbones. However, as discussed previously the contrast between chains is limited because they interpentrate, and from the position of the polymerization peak it would also appear that more than one chain is associated with this interunit peak. Additionally, it is difficult to envisage how the diameter at the chain backbone would expand in step with the increased separation. Rather, it appears that the electron density constrast, which is responsible for the polymerization peak is associated with a localized region of low electron density corresponding to each 'lattice' point. By analogy with the crystal structure of i-PS, this feature is assigned as the low density core in the centre of aggregates of phenyl groups (*Figure 13*). The very

localized nature of these regions of low electron density means that they will undergo proportionally large changes in size as the spacing of the chains changes with temperature. Hence, based on the rationale that the (electron deficient) units may be dilute and increase in size with increasing temperature, it is worthwhile to calculate the intensity changes expected. To do this requires a model, and the fact that the polymerization peak intensifies onto the equator for oriented samples suggests that these small regions have an anisotropic shape. Accordingly a first model will comprise a small group of 7 parallel cylinders, packed in a hexagonal arrangement, the overall size probably being smaller than the extent of spatial correlations in PS. The scattering for such an assemblage of cylinders has been given in analytical form by Vainshtein[44]:

$$I(s) = F_c^2(s).T(s)$$

where $F_c(s)$ is the cylinder scattering factor and $T(s)$ is the interference function.

T is dependent on both s and the intercylinder distance R and, hence, is rexpressed as a function of u, where $u = Rs$, and J_0 denotes a zero-order Bessel function by:

$$T(u) = 1/4a[(7 + 24J_0(u) + 12J_0(u\sqrt{3}) + (J_0(2u)]$$

The intercylinder distances R_t were obtained by interpreting the results of Kilian *et al.*[18] using a modified Bragg Law.

The cylinder radius was set:

$$r_{cyl} = r_0 + r_t$$

with r_t assigned as the increment of the Bragg spacing above that at room temperature. *Figure 20* shows the results of these calculations for a range of values of r_0. The rate of intensity increase is determined by the initial size of the electron density core or hole, as indicated with the previous curves. Using this model a core size of 1 Å is predicted. Of course there are other factors to take into account, particularly the smearing of the electron density about each hole, and thus the value suggested here for the core size is probably an upper limit. Nevertheless, these calculations demonstrate that the marked intensity increase observed in PS may be related to expanding holes which are of a size similar to that of the core of a stack of micro-segregated phenyls.

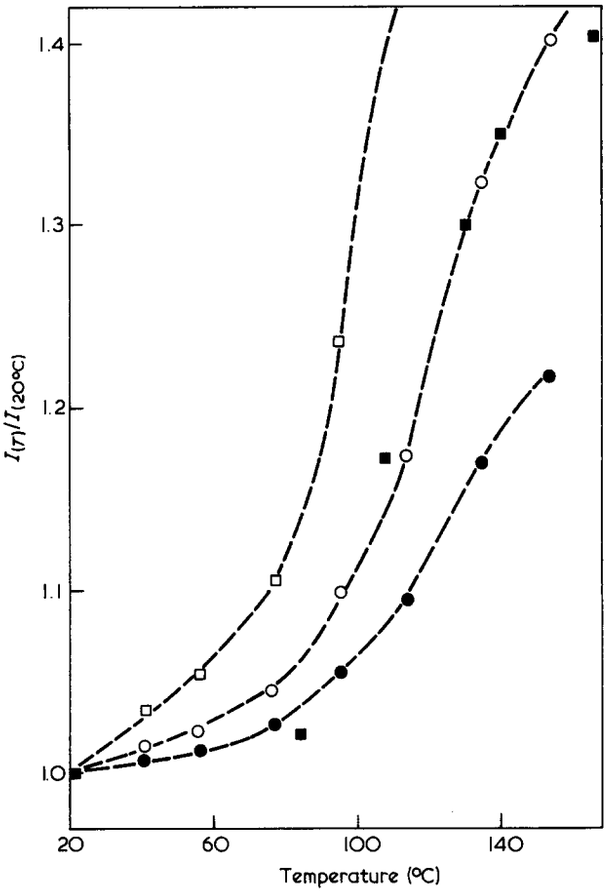

Figure 20 The calculated intensity variation with temperature, for an expanding system of seven parallel cylinders. The dashed lines represent the results for initially different cylinder radii. r_0: □, 0.5 Å; ○, 1.0 Å; ●, 1.5 Å. ■, Experimental results[42]

THE SUPERCHAIN MODEL

The analysis of the WAXS scattering of non-crystalline polystyrene indicates several structural features which would need to be incorporated in an appropriate model. The scattering at values of $s > 1.5$ Å^{-1} indicates that the polymer backbone assumes no persistent conformation. It is dominated by the consequence of interphenyl correlations which are very similar to those associated with the short-range packing of such groups in liquid benzene or styrene. The polymerization peak is, compared with equivalent peaks in many other non-crystalline polymers, at an unusually small scattering angle, comparatively weak, and shows unusual thermal behaviour in that it markedly increases in intensity with increasing temperature. It has been shown that these scattering features can only be accounted for if the phenyl side groups segregate on a molecular scale into stacks. Thus, it appears that in the non-crystalline state, the structure contains phenyl stacks with narrow cores of low electron density, which are highly disordered versions of those which feature in the crystal structure of isotactic PS. The nature of the disorder is significant. In quenched i-PS the backbones appear to be approximately three-fold co-ordinated which would imply that each stack would contain phenyl groups from six different molecules. However, unlike the i-PS crystal, the backbone is not in a regular 3/1 helical conformation; thus, there is no reason to suppose that the phenyls associated with one backbone will be distributed amongst the three associated stacks in an orderly sequence. It is presumably the requirement of correct stack sequencing for crystallization which renders that process comparatively slow in i-PS despite the high flexibility of individual molecules.

In a-PS, the backbone coordination number appears to be between three and four, and again there is no reason to suppose that the distribution of the phenyls into the neighbouring stacks will be regularly sequenced, especially in view of the relatively low chemical order associated with the presence of 60% racemic dyads. The irregular distribution of phenyl groups into stacks will also lead to a high level of positional and rotational disorder of the groups within any stack. Again, whereas the phenyl stacks in the i-PS crystal are parallel, it should be emphasized that for non-crystalline polystyrene there is *no* evidence that the stacks are straight on any scale

significantly larger than their diameters. Thus, although there is strong evidence for the existence of stacks there is no indication of any longer-ranger order. It may be useful to consider the stacks as having features of random coil packing, with the very much thinner backbones roaming between them and of course cross-linking them together. These features are depicted in *Figure 21* with the stacks assuming the role of superchains.

ADDITIONAL INFORMATION

So far, the extra information available in the WAXS from oriented samples has only been used qualitatively. In particular, it has served to identify the lowest angle peak at $s=0.75$ Å^{-1} as interchain, as it intensifies on the equator on drawing. One quantitative aspect, is the observation that as the sample is oriented[16], the interchain peak changes in neither width nor, when geometric factors are taken into account, intensity. Thus, it appears that the phenyls are stacked as superchains in the unoriented material, and the possibility that they are grouped into spheroidal regions which only form into superchains on orientation can be eliminated.

It is possible to azimuthally sharpen the CDF of *Figure 3* to reveal further details as in *Figure 22*. Even considering that the sharpened CDF represents an auto-convolution of the actual structure, the regularity in the positions of the maxima is marked.

In accordance with the previous arguments based on comparisons with the scattering from benzene and styrene, the CDF is seen to be dominated by inter-phenyl information. The weak equatorial peak, so important in understanding the packing between the chain molecules, has relatively little influence on the CDF, although it is probably responsible for the fact that the maxima positioned 10 Å from the meridional axis are as strong, if not stronger than those only 5 Å from this axis. Assuming, therefore, that it is sensible to ascribe the maxima to the positions of phenyl groups, there are several points of note. Firstly, the repeat along the chain axis is of the order of 5 Å, whereas that normal to the axis is ≈9 Å. In part, this difference can be associated with the contribution of the chain backbone thickness to the lateral spacing, but

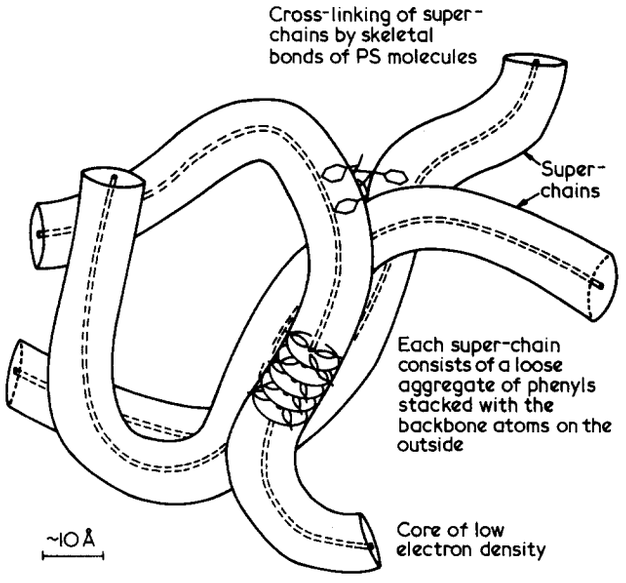

Figure 21 The essential features of the superchain model

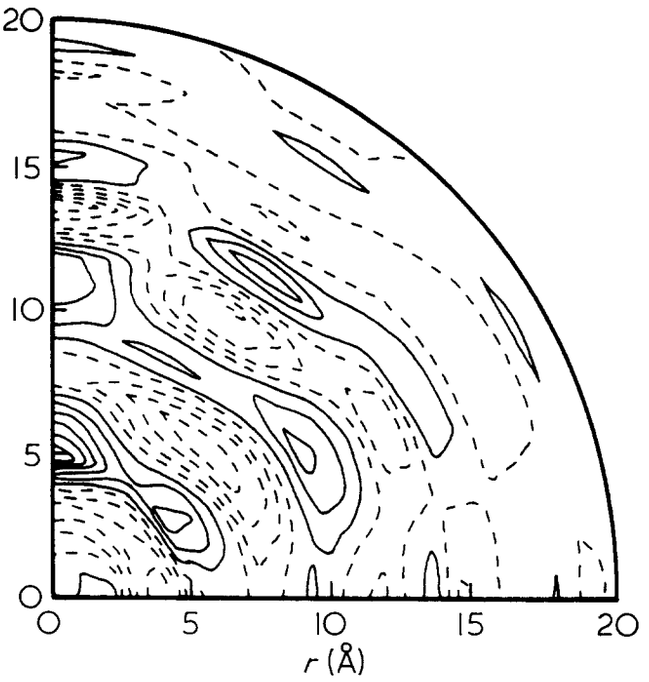

Figure 22 The experimentally derived CDF for a-PS azimuthally sharpened using an orientation distribution function obtained from the arcing of the of the polymerization ring[9]

there may also be some tendency for the planes of the phenyl's to lie normal to the chain axis. The lateral correlation persists to approximately 15 Å which demonstrates that there is significant positional register not only between the phenyl groups in one stack but between such groups in neighbouring stacks. Once again, however, it must be emphasized that the correlations are not long range in the accepted meaning of the term.

CONCLUSIONS

X-ray scattering from non-crystalline polystyrene at angles beyond $s=1.0$ Å^{-1} is very similar to that from benzene and styrene. It is dominated by inter-phenyl correlations which are *inter* as well as *intra* chain. For this reason previous attempts to model the scattering with isolated chains have been unsuccessful. The peak in the scattering at $s=0.75$ Å^{-1} concentrates on the equator for oriented specimens and is thus identified with interchain correlations. However, compared with several other non-crystalline polymers, it is unusual in several respects. It is comparatively weak at room temperature and, considering the likely dimensions of a polystyrene molecule, at a surprisingly low angle. It also increases rapidly in intensity with increasing temperature. The special nature of this peak indicates that the phenyl groups of neighbouring molecules undergo a form of microsegregation whereby they are associated in stacks; there being half as many stacks as chains, although as many as six molecular chain segments may contribute phenyls to the same region of a stack. The rapid increase in peak intensity with temperature has been shown to be a consequence of the nature of the stacks in that there is a narrow, comparatively electron deficient, core at their centres. The narrowness of the core means that its proportional increase in area as a consequence of general thermal expansion is considerable, and the increase in peak intensity correspondingly large. The fact that most of the X-ray

scattering comes from phenyl groups encourages one to think of the stacks as 'superchains', the packing of which is described by the peak at 0.75 $Å^{-1}$. The generation of a cylindrical distribution function from oriented data indicates a short-range regularity in the relative disposition of phenyl groups which extends over distances in excess of the diameter of one stack.

The microsegregation of phenyls into stacks is also a feature of the crystal structure of isotactic polystyrene as described by Natta. However, in the crystal the stacking of phenyls is, of course, completely regular and the comparatively slow crystallization rate of the isotactic polymer can be seen as a consequence of the necessary rearrangements of the position of phenyls both within and amongst the stacks. The arrangements of phenyls in the stacks also tends to interlock neighbouring molecules, and will be disturbed by mechanical plastic deformation. It is possible that the very narrow shear bands seen in deformed polystyrene glasses represent regions where the interlocking has been partially destroyed thus encouraging further concentration of slip.

ACKNOWLEDGEMENTS

The authors wish to thank SERC for funds, Professor R. W. K. Honeycombe FRS for the provision of facilities and Mrs C. E. Bishop who processed a particularly tortuous manuscript.

REFERENCES

1 Katz, J. R., Selman, J. and Heyne, L. *Z. Kautschuk* 1927, 217
2 Katz, J. R. *Trans. Faraday Soc.* 1936, **32** 77
3 Huhnemorder, M. *Z. Kautschuk* 1922, **106**, 126
4 Wecker, S. M., Davidson, T. and Cohen, J. B. *J. Mater. Sci.* 1972, **7**, 1249
5 Adams, R., Balyuzi, H. H. and Burge, R. E. *J. Mater. Sci.* 1978, **13**, 391
6 Lovell, R., Mitchell, G. R. and Windle, A. H. *Faraday Disc.* 1979, **68**, 46
7 Johnson, L. F., Heatley, F. and Bovey, F. A. *Macromolecules* 1970, **3**, 175
8 Waring, J. R., Lovell, R., Mitchell, G. R. and Windle, A. H. *J. Mater. Sci.* 1982, **17**, 1171
9 Mitchell, G. R. and Lovell, R. *Acta Cryst.* 1981, **A37**, 487
10 Lovell R. and Windle A. H. *Polymer* 1981, **22**, 175
11 Mitchell, G. R., Lovell, R. and Windle, A. H. *Polymer* 1982, **23**, 1273
12 Milberg, M. E. *J. Polym. Sci. A-1* 1966, **4**, 801
13 Brady, T. E. and Yeh, G. S. Y. *J. Macromol. Sci. Phys.* 1973, **B7**, 243
14 May, M. and Wattho, C. *Plast. Kaufschuk* 1974, **21**, 367
15 May, M. *J. Polym. Sci. Symp.* 1977, **58**, 23
16 Colebrooke, A. and Windle, A. H. *J. Macromol. Sci. Phys.* 1976, **B12**, 373
17 Lovell R. and Windle A. H. *Polymer* 1976, **17**, 488
18 Kilian, H. G. and Boueke, K. *J. Polym. Sci.* 1962, **58**, 311
19 Krimm, S. *J. Phys. Chem.* 1953, **57**, 22
20 Schuback, H. R., Nagy, E. and Heiss, B. *Colloid Polym. Sci.* 1981, **259**, 789
21 Ino, T. *J. Phys. Soc. Japan* 1953, **8**, 92
22 Katuda, K. *Acta Cryst.* 1963, **16**, 290
23 Bjornhaug, A., Ellefsen, O. and Tonnesen, B. A. *J. Polym. Sci.* 1954, **12**, 621
24 Gupta, M. R. and Yeh, G. S. Y. *J. Macromol. Sci. Phys.* 1978, **B15**, 119
25 Yoon, D. Y., Sundararajan, P. R. and Flory, P. J. *Macromolecules* 1975, **8**, 776
26 Cotton, J. P., Decker, D., Benoit, H., Farnoux, B., Higgins, J., Janninck, G., Ober, R., Picot, C. and de Cloizeaux, J. *Macromolecules* 1974, **7**, 863
27 Wignall, G. D., Ballard, D. G. H. and Schelten, J. *Europ. Polym. J.* 1974, **10**, 861
28 Dettenmaier M. and Fischer, E. W. *Macromol. Chemie* 1976, **17A**, 1185
29 Liquori, A. M. and de Santis, P. *J. Polym. Sci.* 1969, **C16**, 1583
30 Panov, V. P., Gusev, V. V. and Yeudakev, V. P. *Polym. Sci. USSR*, 1974, **16**, 2442
31 Beck, L. and Hagele, P. C. *Colloid Polym. Sci.* 1976, **254**, 228
32 Stegen, G. E. and Boyd, R. H. *Polym. Preprints* 1978, **19**, 595
33 Abe, A., Tonelli, A. E. and Flory, P. J. *Macromolecules* 1970, **3**, 294
34 Tonelli, A. E. *Macromolecules* 1973, **6**, 682
35 Natta, G., Corradini, P. and Bassi, I. W. *Nuovo Cumento Suppl.* **15**, 65.
36 Atkins, E. D. T., Isaac, D. H., Keller, A. and Miyasaka, K. *J. Polym. Sci. Polym. Phys. Edn.* 1977, **15**, 261
37 Flory, P. J. 'Statistical Mechanics of Chain Molecules', Interscience, New York, 1969
38 Yoon, D. Y. and Flory, P. J. *Macromolecules* 1976, **9**, 929
39 Mitchell, G. R., Lovell, R. and Windle, A. H. *Polymer*, 1980, **21**, 989
40 Narten, A. H. *J. Chem. Phys.* 1977, **67**, 2102
41 Waring, J. R. *Thesis*, University of Cambridge, 1979
42 Lovell, R. unpublished work
43 Guinier, A. and Fournet, G. 'Small-angle scattering of X-rays', John Wiley, New York, 1955, Chap. 2
44 Vainshtein, B. K. 'Diffraction of X-rays by Chain Molecules', Elsevier, Amsterdam, 1966